ORIENTAL JOURNAL OF CHEMISTRY
An International Open Access, Peer Reviewed Research Journal
www.orientjchem.org
ISSN: 0970-020 X
CODEN: OJCHEG
2024, Vol. 40, No.(5):
Pg. 1313-1319

Green and Eco-friendly Adsorption of Tetracycline using Nano Sized *Moringa oleifera*: Thermodynamic and Kinetic Studies

NASER NIKMARAM[1], HAMED ESLAMI[2], ALI KHANZADEH POSHTIRI[3], FATEMEH ZISTI[4], DAVOUD BALARAK[5]* and KETHINENI CHANDRIKA[6]

[1]Department of Environmental Engineering, Azad university west Tehran branch, Tehran, Iran.
[2]Department of Chemical, Petroleum and Gas Engineering, Semnan University, Semnan, Iran.
[3]Department of Natural Science, Gorgan University of agriculture and natural science, Gorgan, Iran.
[4]Department of Chemistry, University of Brock, St. Chatarines, Ontario, Canada.
[5]Department of Environmental Health, Health Promotion Research Center, Zahedan University of Medical Sciences, Zahedan, Iran.
[6]Department of Biotechnology, Koneru Lakshmaiah Education Foundation, Guntur, India.
*Corresponding author E-mail: dbalarak2@gmail.com

http://dx.doi.org/10.13005/ojc/400513

(Received: July 29, 2024; Accepted: September 18, 2024)

ABSTRACT

The extensive use of antibiotics in medicine for human and animals has led to the direct or indirect entrance of these chemicals into the environment, especially water bodies. Present research involves the production of low-cost nano-sized *Moringa oleifera* (NSMO) for examining the thermodynamics of tetracycline (TC) adsorption from aqueous solutions. Adsorption experiments in batches were carried out to investigate how contact time (ranging from 10 to 120 min) and solution temperatures (15, 30, and 45 degrees) at a constant pH of 7 affect TC removal. The findings from this research specified that the TC adsorption by the NSMO rises with increasing mixing time and temperature, suggesting that the process is of an endothermic nature. At an optimal contact time of 90 minutes and a temperature of 45°C, a maximum of 99.1% of TC (25 mg/L) was removed. This research demonstrates that NSMO serves as an accessible, cost-effective, and efficient biosorbent that is also environmentally friendly for eliminating TC from aqueous solutions.

Keywords: Tetracycline, Biosorption, Thermodynamics, *Moringa oleifera.*

INTRODUCTION

Environmental pollution caused by industrial waste is a significant concern in recent times.[1,2] Antibiotics have played a crucial role in saving lives over the years by effectively treating bacterial infections.[3] Scientists are actively seeking additional antibacterial chemical compounds, although they face limitations due to potential adverse effects.[4,5] The surge in antibiotic usage, driven by a growing global population, underscores the urgent need for improved medications. Furthermore, the non-medical utilization of antibiotics significantly contributes to their consumption.[6,7] Notably, antibiotics remain

partially undigested after ingestion, leading to their detection in sewage systems.[2] Unfortunately, these undigested antibiotics often prove non-biodegradable, rendering photolysis ineffective against them.[8,9]

The metabolism of certain antibiotics leads to their elimination through feces, while the non-biodegradable remnants accumulate in the environment. This accumulation is a factor in the rise of antibiotic-resistant bacteria.[10,11] As a consequence, thousands of people are lost annually worldwide as a result of antibiotic-resistant bacteria.[12] The levels of antimicrobial resistance in drinking water are lower in comparison to those measured in various effluents, including pharmaceutical emissions, agricultural water, and hospital discharges[13,14] Pharmaceutical companies and inadequate industrial wastewater treatment further intensify the manifestation of antibiotics within the environment.[15] The latest research shows that lactams, quinolones, ionophores, quinolones, ionophores, sulfonamides, and tetracyclines are readily adsorbed yet resistant to degradation.[16] The antecedent incidence of these types of the pharmaceutics in drinking water to the escalation of antibiotic-resistant bacteria and their transmission to animal and human pathogens is not effectively addressed by conventional treatment plants, treating only 48–77% of this issue and leading to significant hygienic and quantifiable clinical risks.[17,18] Despite the limitations of existing treatment technologies in completely resolving the issues, tackling it at its source can alleviate extra ecosystem contamination.[19] Owing to their vast diversity and comprehensive classification, special procedures are necessary to separate antibiotics from wastewater.[20]

Numerous approaches have been utilized to abolish antibiotics from wastewater, e.g., electrochemical degradation, photocatalytic degradation, sonochemical degradation, cation exchange membranes, ultrafiltration, integrated chemical-biological degradation, adsorption/precipitation processes, and adsorption on activated carbon.[21-23]

Adsorption is typically considered the most efficient technique for wastewater treatment among these options, given its affordability, high efficiency, minimal generation of chemical and/or biological sludge, potential for biosorbent regeneration, ease of operation, and enhanced effectiveness.[8,9] While activated carbon appears to be an effective adsorbent, its operational costs are high.[24] Therefore, many studies have shown that alternative adsorbents, e.g., agricultural waste including Canola, Lemna minor, *Azolla filiculoides*, banana shell, Coconut shell, and Rice hull, are utilized for efficient wastewater treatment.[25-27]

Moringa oleifera (MO) is frequently used in the process of purifying water to eliminate pollutants. This is due to its functional groups (i.e., hydroxyl, carboxyl, amines, and phenolic groups), which contribute to its ability to adsorb organic materials.[28] It is the most commonly cultivated species within the Moringa genus. Numerous studies on MO focus on its pharmacological properties.[29,30]

The study's significance lies in its potential to address a pressing environmental issue: antibiotic contamination in water bodies. The overuse of antibiotics has led to their presence in the environment, posing risks to aquatic ecosystems and human health. The use of *Moringa oleifera*, a widely available and relatively inexpensive plant, for producing the nanosorbent (NSMO) makes it a cost-effective alternative to traditional water treatment methods. The aim of this research is to transform agricultural waste into valuable biosorbents with economic value for eliminating tetracycline (TC) from water-based solutions.

MATERIALS AND METHODS

TC was acquired from Sigma Aldrich, Inc (Fig. 1). TC stock solution (1000 mg/L) were formulated by dissolving precisely measured TC in distilled water, and experimental solution concentrations were adjusted through dilution.

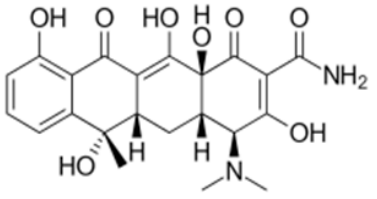

Fig. 1. Chemical structure of TC

Moringa oleifera (MO) leaves were gathered from the Medicinal Agriculture Research Center in Sari, Iran. Samples of MO powder were processed to nano size using a Mill MS Micro-Grinding Mixing technique.

In the batch system, adsorption experiments were accomplished at different temperatures. In each 200 mL leak-proof Corning reagent bottle, 100 mL of the TC solution was poured. The required quantity of adsorbent was accurately measured and moved to each bottle. The bottles were put into a mechanical shaker and shaken vigorously for the designated time (90 minutes). Following the shaking, the flask was left undisturbed to allow the adsorbent to settle, and a sample was extracted from the flask and spun in a centrifuge. The equilibrium concentration of the filtrate was determined using the standard curve, following standard procedures.

The absorbance of each TC solution sample was gauged using a UV/Visible-spectrophotometer at the initiation and termination of the experiment, at λ_{max} = 582nm. The quantity of adsorbate adsorbed at equilibrium, q_e (mg/g), was determined through employment of below equation.[31]

$$q_e = \frac{(Co - Ce) \times V}{M} \quad (1)$$

In the equation, C_0 and C_e (mg/L) denote the initial and equilibrium concentrations, respectively, of the TC in the liquid phase. M represents the utilized adsorbent mass (measured in g), while V indicates the solution volume (measured in L).

To better grasp the TC adsorption process using NSMO, we computed changes in standard enthalpy (ΔH^o), standard entropy (ΔS^o), and standard Gibbs free energy (ΔG^o), i.e., thermodynamic parameters. The Gibbs free energy change can be determined at constant temperature using the Van't Hoff expression, as illustrated in the following equations.[32]

$$K_c = \frac{q_e}{C_e} \quad (2)$$

$$\Delta G^o = - RT \ln K_c \quad (3)$$

$$\ln K_c = \frac{\Delta S^0}{R} - \frac{\Delta H^0}{RT} \quad (4)$$

Adsorption kinetics

The examination of the mechanisms controlling the TC adsorption onto NSMO involved applying the models of PFO, PSO, and IPD to the experimental equilibrium data. The non-linear forms of the PFO and PSO as Equations (5) and (6) are as follows:[33,34]

$$\log(q_e - q_t) = \log(q_e) - \frac{k_1}{2{,}303} t \quad (5)$$

$$\frac{t}{q_t} = \frac{1}{k_2 . q_e^2} + \frac{1}{q_e} t \quad (6)$$

The quantities q_e and q_t represent the amount adsorbed (mg/g) at equilibrium and at time t (min), respectively. The adsorption rate constant of the PFO and PSO are denoted as k_1 (min^{-1}) and k_2 ($g.mg^{-1}\ min^{-1}$), respectively.

The IPD can be described as:[35]

$$q_t = k\, t^{0.5} + C \quad (7)$$

The quantity of solute adsorbed per gram of adsorbent (mg/g) at time t (min) is represented by the symbol q_t. The parameter k denotes the adsorption rate constant of the IPD, and C denotes a constant that corresponds to the thickness of the boundary layer.

RESULTS AND DISCUSSION

The SEM images revealed the initial morphologies of NSMO prior to TC adsorption. Fig. 2a shows that the surface of NSMO was uneven, with elliptic cylinder channels scattered across it. The N_2 adsorption-desorption curve of NSMO, following IUPAC classification, was categorized as a type IV isotherm with a type H_4 hysteresis loop, suggesting mesopores (Fig. 2b). This verified mesoporous nature of NSMO (an average pore diameter = 4.47nm and SBET = 124.2 m^2/g) (Fig. 2c). It can be concluded that TC molecules were capable of passing through the pores of the NSMO structure (maximum diameter of TC = 12.7 Å).

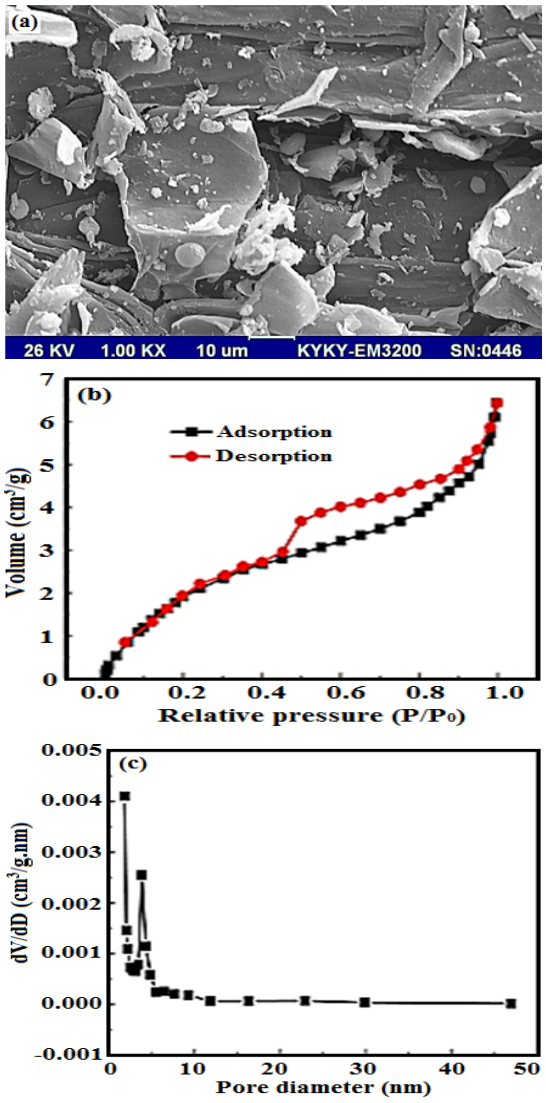

Fig. 2. SEM image of biosorbent NSMO (a); N_2 adsorption and desorption isotherms (b) pore size distribution (c)

How temperature and contact time affect the TC adsorption by NSMO were simultaneously explored across different temperature ranges (288, 303, and 318 K) and contact times (10-120 min) at a natural pH of 7 (Figure 3).

Thermodynamic parameters (i.e., ΔG^o, ΔH^o, and ΔS^o) were appraised to comprehend the feasibility and nature of the studied process (Table 1).

In our investigation, kinetic models were applied to selected TC concentrations at a pH of 5 and NSMO mass of 1 g/L. The R^2 values and parameters estimated by three kinetic models are detailed in Table 2. Based on the data in the table and as depicted in Fig. 4a-b, the R^2 of the PSO model was found to be higher compared to the PFO models. The Q_e obtained from the PSO is, furthermore, in better alignment with the experimental equilibrium adsorption capacity.

In Fig. 4b, the graphs of Qt versus $t^{0.5}$ resulting from the adsorption of TC onto NSMO for various concentrations were illustrated; this representation helps to elucidate the involvement of multiple steps in the adsorption process. The mechanism and steps that restrict the rate of TC adsorption were determined using both the IPD model and the LFD model. Throughout the process, the transportation of TC molecules was affected one of the above-mentioned diffusion models, or a blend of them. In Fig. 4c, the multilinear graphs of q_t versus $t^{1/2}$, which are obtained at 10, 25, 50, and 100 mg/L TC are represented. The values required for the IPD, such as kp, Ci, and R^2, are presented in Table 2. The IPD constant, kp, is associated with the straight line's slope, while C is linked to the thickness of the boundary layer.

Table 1: Thermodynamic values for the TC adsorption process by NSMO

Temperature (K)	ΔG^0 (KJ/mol)	ΔH^0 (KJ/mol)	ΔS^0 (KJ/mol K)
288	-2.11		
303	-4.23	33.77	0.321
318	-6.02		

Table 2: Parameters obtained from kinetic studies

	$Q_{e,exp}$	24.1	56.4	81.2	107.4
PFO	C_O	10	25	50	100
	K_1	0.029	0.034	0.071	0.0654
	$q_{e,cal}$	6.92	23.7	39.2	48.7
	R^2	0.905	0.874	0.724	0.617
PSO	K_s	0.001	0.003	0.006	0.007
	$q_{e,exp}$	21.4	52.3	78.2	99.5
	R^2	0.977	0.999	0.998	0.981
IPD	Stage 1				
	K_1	2.75	4.35	8.13	13.4
	C	1.65	3.27	5.19	8.29
	R^2	0.934	0.953	0.923	0.915
	Stage 2				
	K_2	1.09	2.11	2.76	4.17
	C	4.26	11.2	18.6	22.3
	R^2	0.973	0.978	0.991	0.986
	Stage 3				
	K_3	0.071	0.128	0.173	0.424
	C	2 8.1	15.1	23.2	31.5
	R^2	0.914	0.921	0.917	0.954

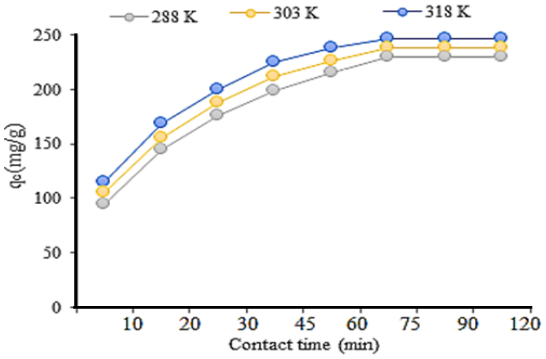

Fig. 3. Effect of contact time and temperature on capacity adsorption

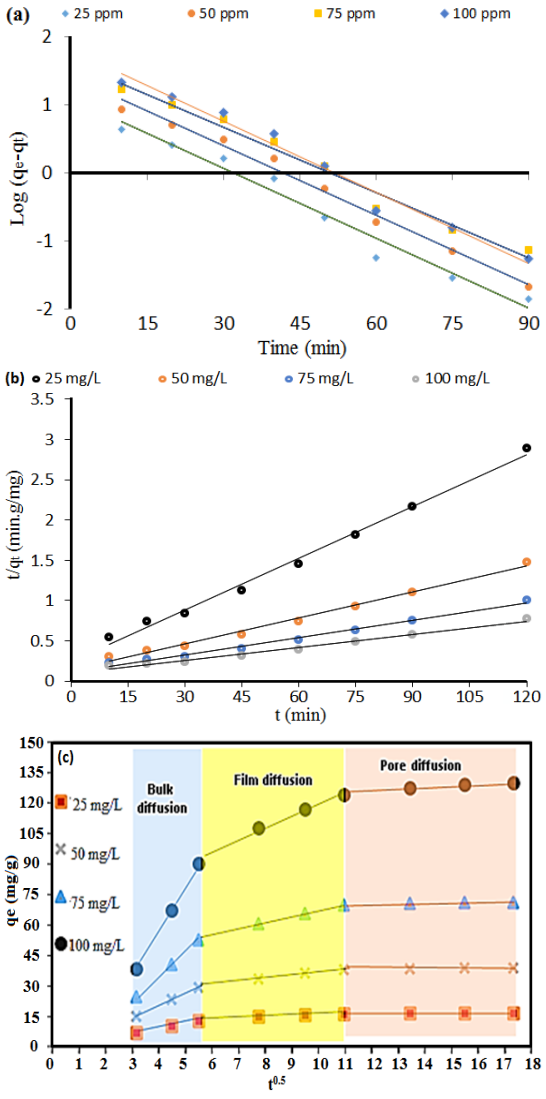

Fig. 4. Kinetics of TC adsorption. PFO (a) PSO (b) IPD (c)

The adsorption of TC antibiotics onto the NSMO rises as the duration of contact and temperature rise, suggesting that the process is of an endothermic nature. It could be attributed to the heightened movement of the TC molecules and an augmented number of active sites for adsorption as the temperature increases.[36]

The TC adsorption process onto the NSMO was confirmed to be thermodynamically feasible and spontaneous at all temperatures (288, 303, and 318 K) by $\Delta G^{o}<0$.[37] The verification of the process's endothermic nature was confirmed by the positive ΔH^{o} value.[38] The raised level of randomness at the solid-liquid interface during TC adsorption by NSMO was suggested by the positive ΔS^{o} value.[39]

To shed light on how the electrostatic attraction stimuluses TC adsorption by NSMO, the dependency on pH levels was examined. Despite the pH increase from 3.0 to 7.0 resulting in only a 4% decrease in adsorbed TC, further escalation to pH 11 induced a significant 27% reduction in adsorption. This trend can be elucidated by TC's amphiphilic properties, which allow its existence in aqueous solution as cations (TCH_3^+), zwitterions (TCH_2^+), and anions (TCH_2^-).[25] As pH rises, TC undergoes a gradual transition from being cationic to anionic. Upon reaching the isoelectric point of NSMO (pHpzc=6.7), the interaction between studied pollutant and NSMO changes from weak to strong. Moreover, the increase in pH levels causes the amino and phenolic hydroxyl groups on TC's surface to lose a proton, which then prevents potential interactions between TC and the graphitized structure of NSMO, such as π-π and cation-π electron donor-acceptor (EDA) interactions. As a result, this leads to a further reduction in the adsorption quantity.[15] Yet, the adsorption capacity remained above 142.5 mg/g within the pH from 3 to 7. This suggests that electrostatic attraction may not be the primary adsorption mechanism, a notion further supported by minimal effect of ionic strength on the adsorption process. Similarly, in acidic conditions, the adsorption capacity exhibited little variation with pH, indicating that hydrogen bonding also was not a key factor in the interaction.[40]

The adsorption experiments conducted at different temperatures are segmented into three periods, marked by three successive straight lines obtained by fitting adsorption models to the data. In the first period, adsorption is governed by liquid film

diffusion, involving the transfer of TC molecules from the liquid phase to the NSMO surface.[41] During this step, adsorption proceeded more rapidly compared to the subsequent steps. In the plots for the initial step, corresponding to adsorption concentrations of 10, 25, 50, and 100 mg/L, the fittings did not intersect the origin, pointing towards intraparticle diffusion not being the sole determinant of the adsorption process's rate.[42] Throughout the second, the second step, the pores of the NSMO particles were slowly filled with pollutant molecules, leading to an IPD rate-limiting step. During final step, the advancement slowed (TC concentration remaining in the solution is less in this step), presumed to be approaching adsorption equilibrium. The values of kp for two last stages showed a decrease relative to the first stage, indicating the deceleration of IPD as the TC concentration in the solution diminished.[43-45]

It is essential to consider the adsorbent dose as it contains numerous hollow active sites that capture pollutants. The ideal dose to achieve the highest TC adsorption rate is 1 g/L. The lower qe at high doses may be described based on the possibility that an excessive amount of adsorbent could impede pollutant movement. In large adsorbent quantities, adsorbent particles might aggregate, hindering antibiotic transport to the adsorption sites. As a result, the interaction between the antibiotic and adsorbent decreases, which lowers the adsorption rate. Conversely, at lower doses, the likelihood of adsorbent accumulation is less while the possibility of TC adsorption onto the adsorbent surface is enhanced.[46]

CONCLUSION

The adsorption of TC onto the NSMO was examined through thermodynamic studies. The analysis of the thermodynamics revealed that the adsorption process occurred spontaneously, as indicated by the negative standard Gibbs free energy change (ΔG^o). Furthermore, the changes in entropy (ΔH^o) and enthalpy (ΔS^o) were determined to be 9.84 kJ/mol and 0.0184 kJ/mol K, respectively. The predominant mode of TC adsorption by NSMO is chemical adsorption. These processes contribute to the exceptional adsorption performance of NSMO and offer insights for the design of highly efficient adsorbent materials. Overall, NSMO stands out as an extremely efficient adsorbent with swift adsorption and concise adsorption periods, making it apt for batch systems. Additionally, it is effective, environmentally friendly, non-toxic, easily retrievable, and capable of eliminating antibiotic pollution from water.

ACKNOWLEDGEMENT

The authors extend their appreciation to Zahedan university of medical sciences for their support of this research (IR.ZAUMS.REC.1401.147).

Conflict of Interest

The authors declare no conflict of interest.

REFERENCES

1. Balarak, D.; Ganji, F.; Chandrika, K.; Haseeb S., *Int J Pharm Investig.*, **2020**, *10*(2), 122-6.
2. Mostafapour F. K.; Haseeb S.; Balarak D.; Moein H.; Sajadi A. A, Jalalzaei Z., *Int J Pharm Investig.*, **2021**, *11*(1), 41-5.
3. Chang P. H.; Jiang, WT.; Li Z.; Jean, J. S.; Kuo, C. Y., *J. Pharm. Anal.*, **2015**, *4*, 86– 111.
4. Zhang Y.; Zuo S.; Zhou M. Liang L. Ren, G., *Chem. Eng. J.*, **2018**, *335*, 685–692.
5. Zhang P.; Li Y.; Cao Y., *Bioresour. Technol.*, **2019**, *285*, 121348.
6. Cetecioglu Z. Ince B. Azman, S., *Biochem. Biotechnol.*, **2014**, *172*, 631–640.
7. Belaissa Y.; Saib F. Trari.; M., *Reac Kinet Mech Cat.*, **2022**, *135*, 1011–1030.
8. Acosta R.; Fierro V.; De Yuso AM.; Nabarlatz, D., *Chemosphere.*, **2016**, *149*, 168–176.
9. Chen, SQ.; Chen, YL.; Jiang, H., *Ind. Eng. Chem. Res.*, **2017**, *56*, 3059–3066.
10. Bazi, M.; Balarak, D.; Khatibi, A. D.; Siddiqui, S. H.; Mostafapour, F. K., *Int J Pharm Investig.*, **2021**, *11*(3), 269-73.
11. Balarak, D.; Baniasadi, M.; Bazzi, M., *Int J Pharm Investig.*, **2020**, *10*(3), 339-43.
12. Bhadra, B.N.; Seo, P. W.; Jhung, S.H., *Chem. Eng. J.*, **2016**, *301*, 27–34.
13. Zhang, Y., *Environ. Pollut.*, **2021**, *284*, 117537.
14. Lotfi Golsefidi F.; Zahmatkesh Anbarani, M.; Bonyadi, Z., *Appl. Water Sci.*, **2023**, *13*(10), 1–11.
15. Anbarani M. Z.; Ramavandi B.; Bonyadi, Z., *Heliyon.*, **2023**, *9*(3), e14356.
16. Xu B.; Liu F.; Brookes PC. Xu *J. Environ. Pollut.*, **2018**, *240*, 87–94.

17. Mirsoleimani-azizi S. M.; Setoodeh P.; Zeinali S.; Rahimpour, M. R., *J. Environ. Chem. Eng.*, **2018**, *6*(5), 6118–6130.
18. Balarak D.; Azarpira H.; Mostafapour F. K. Inter., *J. Pharm Technol.*, **2016**, *8*(3), 16664-75.
19. Wang Y.; Liu C.; Wang F.; Sun Q., *Chemosphere.,* **2022**, *292*, 133425.
20. El Naga, A.O.A.; El Saied, M.; Shaban, S.A.; El Kady, F. Y., *J.Mol. Liq.*, **2019**, *285*, 9–19.
21. Paul S.C.; Githinji L.J.M.; Ankumah R.O.; Willian K.R.; Pritchett G., *Water Air Soil Pollut.*, **2014**, *38*(225), 1821.
22. Tianyi Shen.; Maria,G.; Chernysheva.; Gennadii, A.; Badun.; Andrey, G., *Popov, Colloids and Interfaces.*, **2022**, *6*(2), 35.
23. Naghsh N.; Chandrika K.; Balarak D., *Int. J. Pharm. Investigation.*, **2024**, *14*(2), 365-70.
24. Álvarez-Torrellas S.; Ribeiro R.; Gomes, HT.; Ovejero, G.; García, J., *Chem. Eng. J.*, **2016**, *296*, 277–288.
25. Li H, Zhang D.; Han X.; Xing, B., *Chemosphere.*, **2014**, *95*, 150–155.
26. Balarak D.; Mostafapour FKv Bazrafshan E.; Saleh T. A., *Water Sci Technol.*, **2017**, *75*, 1599-1606.
27. Reddy, D. H. K; Harinatha Y; Seshaiah, K., *Chem. Eng. J.*, **2010**, *162*, 626-634.
28. Kalavathy M. H; Miranda L. R., *Chem. Eng. J.*, **2010**, *158*, 188-199.
29. Zisti F.; Al-Behadili FJM.; Nadimpour M.; Rahimpoor R.; Mengelizadeh N., *Environ Res.*, **2024**, *245*, 118019.
30. Hettithanthri, O.; Rajapaksha, A. U.; Keerthanan, S., *Chemosphere.*, **2022**, *297*, 133984.
31. Sun Y.; Wang X.; Xia S. Zhao, J., *Chem. Eng. J.*, **2021**, *416*, 129085.
32. Movasaghi, Z.; Yan, B.; Niu, C., *Ind. Crops Prod.*, **2019**, *127*, 237–250.
33. Balarak D.; Taheri Z.; Shim M. J.; Lee S. M.; Jeon C., *Desalin Water Treat.*, **2021**, *215*, 183-193.
34. Balarak, D.; Azarpira, H., *Inter. J. Chem Tech Res.*, **2016**, *9*(7), 566-573.
35. Azarpira H.; Mahdavi Y; Khaleghi, O., *Pharm. Lett.*, **2016**, *8*(11), 107-13.
36. Belhachemi, M.; Djelaila, S., *Environ. Process.,* **2017**, *4*, 549–561.
37. Boukhelkhal, A.; Benkortbi, O.; Hamadeche, M., *Water Air Soil Pollut.*, **2015**, *226*, 323. https://doi.org/10.1007/s11270-015-2587-z.
38. Moarefian, A.; Golestani, H. A. & Bahmanpour, H., *J Environ Health Sci. Engin.*, **2014**, *12*, 127. https://doi.org/10.1186/s40201-014-0127-1.
39. Limousy, L.; Ghouma, I.; Ouederni, A., *Environ Sci Pollut Res.*, **2017**, *24*, 9993–10004. https://doi.org/10.1007/s11356-016-7404-8.
40. Shikuku, V. O., *Appl Water Sci.*, **2018**, *8*, 175. https://doi.org/10.1007/s13201-018-0825-4.
41. Yağmur, H. K.; Kaya., *J. Cryst. Struct.*, **2021**, *1232*, 130071.https://doi.org/10.1016/j.molstruc. 2021.130071
42. Karaer H.; Kaya., *J. Mol. Liq.*, **2017**, *230*, 152–162.
43. Varnaseri, M.; Motahari Zadeh, Z.; Abdolmohammadi, F., *Water Conserv Sci Eng.*, **2024**, *9*, 45. https://doi.org/10.1007/s41101-024-00279-3.
44. Zisti F.; Chandrika K., *Int J Pharm Investigation.*, **2023**, *13*(4), 778–783.
45. Naghsh N.; Barnoos S.; Zisti F.; Chandrika K., *Int J Pharm Investigation.*, **2024**, *14*(2), 365–370.
46. Al-Ha-Wary S.I.S. Gupta R. Sapaev I. B., *Inter. J. Environ. Anal. Chem.*, **2023**, 102-1-11.